Stress Redistribution of a Circular Membrane With a Hole Based on the Mooney-Rivlin Material Model

Michele O. Olivares*[1], Guido David[2]

[1]Division of Physical Sciences and Mathematics, College of Arts and Sciences, University of the Philippines Visayas
[2]Institute of Mathematics, University of the Philippines Diliman, Quezon City

ABSTRACT

The study of deformation in membranes has implications in the field of medicine, mechanobiology, and mechanics. In this study, we consider the case of a thin hyperelastic, incompressible, isotropic membrane with a central hole subjected to outer boundary stretching. The membrane is assumed to follow a quadratic Mooney-Rivlin constitutive relation. Using principles of mechanics and equilibrium equations, the system was formulated, and the resulting boundary value problem is solved using a modified shooting method based on the regula-falsi method. The model is examined numerically for various outer stretches, material parameters, and hole sizes.

KEYWORDS:

finite deformations, mechanotransduction, Mooney-Rivlin material, biomembranes, capsulorhexis, skin biopsy

INTRODUCTION

Solid mechanics is concerned with the deformation and motion of solid materials when subjected to forces. A solid material has the ability to resist tensile, compressive, and shear forces up to elastic limit. When the force is removed, a solid material goes back to its original shape (see Bansal, 2007). Knowledge in solid mechanics is valuable especially in the field of medicine since injuries and clinical procedures are forces that can cause stresses to cells.

Because materials behave differently when subjected to stress, it is very important to study the kinematics of a material undergoing deformations to predict how the material will behave subject to different deformations.

A finite composite laminated plate with an elliptical hole was determined to have a high stress concentration near a hole with larger eccentricity compared to a hole with smaller eccentricity (Xu et al. 1995). In 2004, David and Humphrey studied the redistribution of stress of an isotropic circular membrane which behaves under the Fung model assumption. When a circular hole was introduced to the membrane with a traction-free inner boundary condition, results showed that increasing the size of the hole results in a decrease in the maximum value of the circumferential stress (David and Humphrey, 2004). However, when a zero-displacement condition was applied to the inner boundary of the circular hole of an isotropic circular Fung membrane, the distribution of stress and strain yielded an opposite result from the traction-free condition. Moreover, the radial stress increases as the fixation size increases (Mori et al, 2005).

Rivlin and Thomas (1951) were among the first to study the effects on strain distribution by stretching a thin isotropic sheet, assuming a two-parameter Mooney-Rivlin material model. In this paper, we study the effects on the strain distribution of stretching a Mooney-Rivlin thin isotropic sheet with various hole sizes.

Results of this study may help in the analysis of the effects of stress to cells due to clinical procedures such as skin biopsy and cosmetic surgery. Applications of the study of stresses in membranes with holes include capsulorhexis during cataract surgery (David

*Corresponding Author:
Division of Physical Sciences and Mathematics, College of Arts and Sciences, University of the Philippines Visayas, Miagao (5023), Iloilo;
Email address: moolivares@up.edu.ph

and Humphrey, 2007) and rupture of intracranial saccular aneurysms (David and Nabong, 2015; Nabong and David, 2017).

MATERIALS AND METHODS

Under the principle of hyperelasticity, the introduction of a central hole into an equibiaxially pre-stretched membrane is equivalent to stretching a membrane with a hole. The formulation used in this study follows David and Humphrey (2004). Let a thin circular membrane having a central circular hole be subjected to a uniform radial traction along its outer circumference as shown in Figure 1.

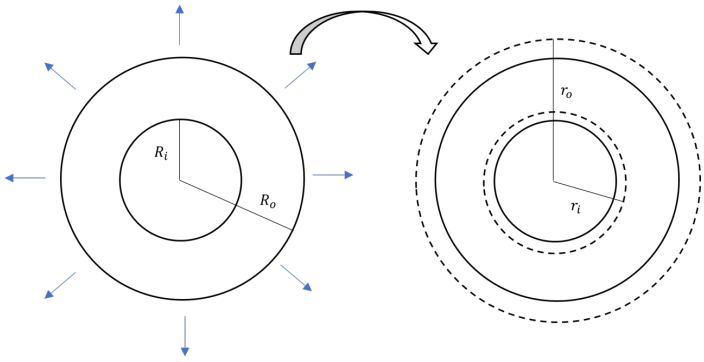

Figure 1. Illustration of a membrane with a hole before and after application of the stretch.

Using cylindrical coordinates, we map the position of a material particle by $(R,\Theta,Z)\rightarrow(r,\theta,z)$ following the application of loads. Moreover, let R_o and R_i be the outer and inner undeformed radii and r_o and r_i be the outer and inner deformed radii. Thus, we can write a motion of the form,

$$r=r(R), \qquad \theta=\Theta, \qquad z=z(Z). \tag{1}$$

The deformation gradient in cylindrical coordinates is now given by

$$\mathbf{F}=\begin{bmatrix} r' & 0 & 0 \\ 0 & \dfrac{r}{R} & 0 \\ 0 & 0 & \dfrac{\partial z}{\partial Z} \end{bmatrix}=\begin{bmatrix} \lambda_R & 0 & 0 \\ 0 & \lambda_\Theta & 0 \\ 0 & 0 & \lambda_Z \end{bmatrix},$$

wherein the λ_i's are the principal stretches and $r'=\dfrac{dr}{dR}$. Assuming that the material is incompressible, (i.e. det **F** =1), then $\lambda_Z=\dfrac{1}{\lambda_R\lambda_\Theta}=\dfrac{R}{rr'}$.

Hence,

$$\mathbf{F}=\begin{bmatrix} r' & 0 & 0 \\ 0 & \dfrac{r}{R} & 0 \\ 0 & 0 & \dfrac{R}{rr'} \end{bmatrix}=\begin{bmatrix} \lambda_R & 0 & 0 \\ 0 & \lambda_\Theta & 0 \\ 0 & 0 & \dfrac{1}{\lambda_R\lambda_\Theta} \end{bmatrix}. \tag{2}$$

The right Cauchy-Green deformation tensor is given by

$$\mathbf{C}=\mathbf{F}^T\mathbf{F}=\begin{bmatrix} \lambda_R^2 & 0 & 0 \\ 0 & \lambda_\Theta^2 & 0 \\ 0 & 0 & \left(\dfrac{1}{\lambda_R\lambda_\Theta}\right)^2 \end{bmatrix} \tag{3}$$

and the Green Lagrange Strain Tensor is

$$\mathbf{E}=\frac{1}{2}(\mathbf{C}-\mathbf{I})=\begin{bmatrix} E_{RR} & 0 & 0 \\ 0 & E_{\Theta\Theta} & 0 \\ 0 & 0 & E_{ZZ} \end{bmatrix}=\frac{1}{2}\begin{bmatrix} \lambda_R^2-1 & 0 & 0 \\ 0 & \lambda_\Theta^2-1 & 0 \\ 0 & 0 & \left(\dfrac{1}{\lambda_R\lambda_\Theta}\right)^2-1 \end{bmatrix}. \tag{4}$$

The generalized Mooney-Rivlin material model for incompressible materials takes the form (Bonet and Wood, 1997; Shabana, 2008)

$$W=\sum_{k=0}^{\infty}\sum_{l=0}^{\infty}c_{kl}(I_1-3)^k(I_2-3)^l, \qquad c_{00}=0$$

where c_{kl}'s are material parameters (coefficients of stiffness) and I_1 and I_2 are invariants of the right Cauchy-Green deformation tensor $\mathbf{C}$ which are given by

$$I_1=\text{tr}\,(\mathbf{C})$$

$$I_2=\frac{1}{2}\{[\text{tr}(\mathbf{C})]^2-\text{tr}(\mathbf{C}^2)\}.$$

In this study, we consider the Mooney-Rivlin material model of the form

$$W=c_{10}(I_1-3)+c_{01}(I_2-3)+c_{20}(I_1-3)^2\,. \tag{5}$$

Restricting the degree of the Mooney-Rivlin model allows the subsequent derivation of the stress-strain relationship easier to calculate.

The nonzero components of the Cauchy stress tensor σ are

$$\sigma_{rr} = \lambda_R^2 \frac{\partial W}{\partial E_{RR}}, \quad \sigma_{\Theta\Theta} = \lambda_\Theta^2 \frac{\partial W}{\partial E_{\Theta\Theta}}, \qquad \sigma_{zz} = \lambda_Z^2 \frac{\partial W}{\partial E_{ZZ}} \tag{6}$$

and all other components are zero.

In the absence of body forces, the only nonzero equilibrium equation is,

$$\frac{\partial \sigma_{rr}}{\partial R} + \frac{1}{r}(\sigma_{rr} - \sigma_{\theta\theta}) = 0. \tag{7}$$

Note that for the motion in Eq. (1),

$$\frac{d\sigma_{rr}}{dR} = \frac{\partial \sigma_{rr}}{\partial r}\frac{\partial r}{\partial R} + \frac{\partial \sigma_{rr}}{\partial \theta}\frac{\partial \theta}{\partial R} + \frac{\partial \sigma_{rr}}{\partial z}\frac{\partial z}{\partial R} = \lambda_R \frac{\partial \sigma_{rr}}{\partial r} \tag{8}$$

and

$$\frac{d\sigma_{rr}}{dR} = \frac{\partial \sigma_{rr}}{\partial \lambda_R}\frac{\partial \lambda_R}{\partial R} + \frac{\partial \sigma_{rr}}{\partial \lambda_\Theta}\frac{\partial \lambda_\Theta}{\partial R}. \tag{9}$$

Taking partial derivatives in Eq. (2), we obtain

$$\frac{\partial \lambda_R}{\partial R} = r'', \quad \text{and} \quad \frac{\partial \lambda_\Theta}{\partial R} = \frac{1}{R}(\lambda_R - \lambda_\Theta). \tag{10}$$

From Eq. (8), we get

$$\frac{\partial \sigma_{rr}}{\partial r} = \frac{1}{\lambda_R}\frac{d\sigma_{rr}}{dR} \tag{11}$$

and using Eqs. (9) and (10),

$$\frac{\partial \sigma_{rr}}{\partial r} = \frac{1}{\lambda_R}\left(r''\frac{\partial \sigma_{rr}}{\partial \lambda_R} + \frac{1}{R}(\lambda_R - \lambda_\Theta)\frac{\partial \sigma_{rr}}{\partial \lambda_\Theta}\right). \tag{12}$$

Substituting Eq. (12) to Eq. (7) and solving for r'', the radial equilibrium equation, which is a second-order ordinary differential equation (ODE) for r, is given by

$$r'' = \frac{\frac{\lambda_R}{r}(\sigma_{\theta\theta} - \sigma_{rr}) + \frac{1}{R}(\lambda_\Theta - \lambda_R)\frac{\partial \sigma_{rr}}{\partial \lambda_\Theta}}{\frac{\partial \sigma_{rr}}{\partial \lambda_R}}, \tag{13}$$

where

$$\sigma_{rr} = 2(r')^2\left[c_{01}\left(\left(\frac{r}{R}\right)^2 - \frac{1}{(r')^4}\right) + c_{10}\left(1 - \frac{R^2}{(r')^4 r^2}\right) + 2c_{20}\left((r')^2 + \left(\frac{r}{R}\right)^2 - 3 - \frac{1}{(r')^4} - \frac{R^4}{(r')^6 r^4} + \frac{3R^2}{(r')^4 r^2}\right)\right]$$

$$\sigma_{\theta\theta} = 2\left(\frac{r}{R}\right)^2\left[c_{01}\left((r')^2 - \left(\frac{R}{r}\right)^4\right) + c_{10}\left(1 - \frac{R^4}{(r')^2 r^4}\right) + 2c_{20}\left((r')^2 + \left(\frac{r}{R}\right)^2 - 3 - \left(\frac{R}{r}\right)^4 - \frac{R^6}{(r')^4 r^6} + \frac{3R^4}{(r')^2 r^4}\right)\right]$$

$$\frac{\partial \sigma_{rr}}{\partial \lambda_\Theta} = 4(r')^2\left(\frac{r}{R}\right)\left[c_{01} + c_{10}\left(\frac{R}{rr'}\right)^4 + 2c_{20}\left(1 + 2\left(\frac{R}{rr'}\right)^6 - 3\left(\frac{R}{rr'}\right)^4\right)\right]$$

$$\frac{\partial \sigma_{rr}}{\partial \lambda_R} = 4(r')\left[c_{01}\left(\left(\frac{r}{R}\right)^2 + \frac{1}{(r')^4}\right) + c_{10}\left(1 + \frac{R^2}{(r')^4 r^2}\right) + 2c_{20}\left(2(r')^2 + \left(\frac{r}{R}\right)^2 - 3 + \frac{1}{(r')^4} + \frac{2R^4}{(r')^6 r^4} - \frac{3R^2}{(r')^4 r^2}\right)\right].$$

Note that r'' is a function of R, r, and r'. To solve the second order ODE, we express it as a system of two first-order ODEs. Denoting $y_1 = r$ and $y_2 = r'$, we obtain the system

$$\frac{dy_1}{dR} = y_2, \qquad \frac{dy_2}{dR} = r''. \tag{14}$$

Solving a second order ODE requires two boundary conditions, either displacement or force boundary conditions. Let σ_o be the uniform radial stress applied on the outer boundary, thus

$$\sigma_{rr}(R_o) = \sigma_o = \lambda_R^2(R_o)\left.\frac{\partial W}{\partial E_{RR}}\right|_{R_o}. \tag{15}$$

The inner boundary is traction free, thus

$$\sigma_{rr}(R_i) = 0 = \lambda_R^2(R_i)\left.\frac{\partial W}{\partial E_{RR}}\right|_{R_i}. \tag{16}$$

From Eq. (16), we can determine the value of the matching derivative given the value for the deformed inner radius.

RESULTS

Given the value of the deformed outer radius, the deformed inner radius was solved using the shooting method based on the regula-falsi method while the governing equation (13) was solved using system (14) using the fourth order Runge–Kutta method.

The range of estimates for the deformed inner radius r_i is between R_i and r_o. This is because the material is incompressible and hyperelastic. Any application of force in the outward radial direction will not cause the inner radius to decrease, thus $r_i \geq R_i$. Secondly, the deformed inner radius cannot exceed the deformed outer radius, i.e. $r_i \leq r_o$. To improve succeeding guesses, we apply the regula-falsi method until a solution is obtained within a tolerance of 10^{-6}.

Consider a circular membrane having a central circular hole with an undeformed outer radius of 2.0 a.u. (units of length are all in arbitrary units or a.u. and are thus dropped for brevity). We obtain numerical results for the following different scenarios: hole sizes of varying radii (0.001, 1.0, and 1.9), different material parameters, and different stretches relative to the undeformed outer radius (5%,10%,15%,20%, and 25%).

The 'pinhole' case is where the undeformed radius of the hole is 0.001 . The 'donut' case is where the undeformed radius of the hole is 1.0, or half the outer radius. The 'thin-ring' case is where the undeformed radius of the hole is 1.9.

For the material parameters, based on some studies using our model, $0 \leq C_{kl} \leq 1$ where C_{kl} is a material parameter in the model (Maurice et al, 2009; Benkahla et al, 2012; Benkahla et al, 2013) but $C_{kl} > 1$ is also possible (Verron and Andriyana, 2008). Since the aim of this study is to help in the analysis of the effects of surgeries and clinical procedures to cells and tissues, we use $0 < C_{kl} < 1$ which is the range of the parameters used for muscle joints in the study of Maurice et al (2009). Although we tested various configurations of material parameters, the general behavior was similar. In these illustrations, we use material parameters c_{01}=0.9, c_{10}=0.2, and c_{20}=0.5.

Figure 2 shows the stress and strain fields for the case of a 'donut' (undeformed hole radius of 1.0) where the outer boundary is stretched 5%, 10%, 15%, 20%, and 25%. Both the circumferential stretch (upper right) and the circumferential stress (lower right) are monotonically decreasing whereas the radial stretch (upper left) and the radial stress (lower left) increase monotonically. The material parameter c_{01} denotes the stiffness in the circumferential direction whereas material parameters c_{10} and c_{20} denote the

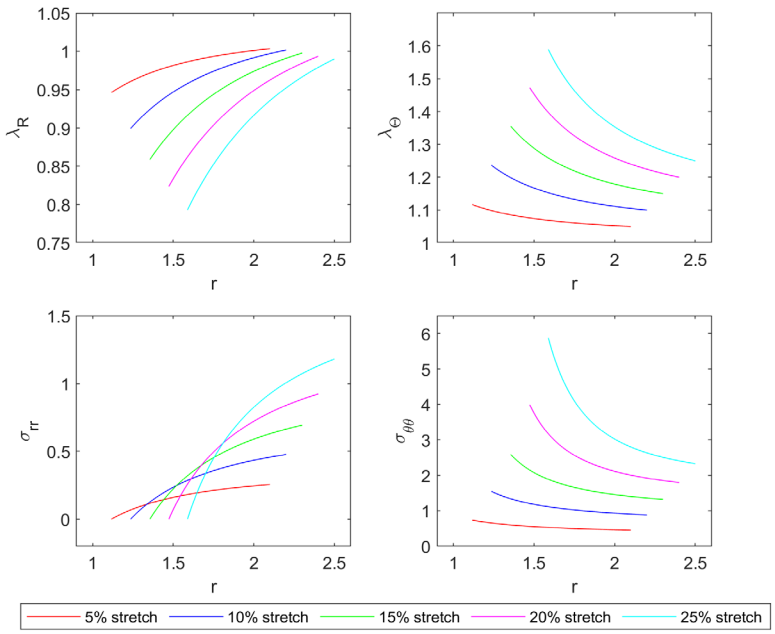

Figure 2. Stresses and strains of a membrane with an undeformed hole size radius of 1.0 and an outer radius of 2.0 extended by 5%, 10%, 15%, 20%, and 25% using parameter values c_{01}=0.9, c_{10}=0.2, and c_{20}=0.5

stiffness in the radial direction in the first and second order, respectively. As the value of c_{01} decreases, the values of the radial stretch at the boundaries increases while the values of the circumferential stretch, circumferential stress, and radial stress at the boundaries decreases. Whereas, increasing c_{10} or c_{20} increases the values of the radial stretch, radial stress, and circumferential stress at the boundaries while decreasing the values of the circumferential stretch at the boundaries.

The stress and strain fields of a membrane with 'pinhole' stretched 5%, 10%, 15%, 20%, and 25% are shown in Figures 3 to 7. The stress is concentrated near the hole and then becomes constant away from the hole. From Figure 8, the stress and strain fields of a 'thin-ring' subjected to 5%, 10%, 15%, 20%, and 25% stretches along the outer boundary exhibit the same behavior as those of a 'donut'.

Results for three membranes with different hole sizes (undeformed hole radius of 0.001, 1.0, and 1.9) subjected to 10% stretch along the outer boundary are shown in Figure 9. A 'pinhole' membrane has high circumferential stress near the hole whereas both the 'donut' and the 'thin-ring' have lower stress concentration near the hole.

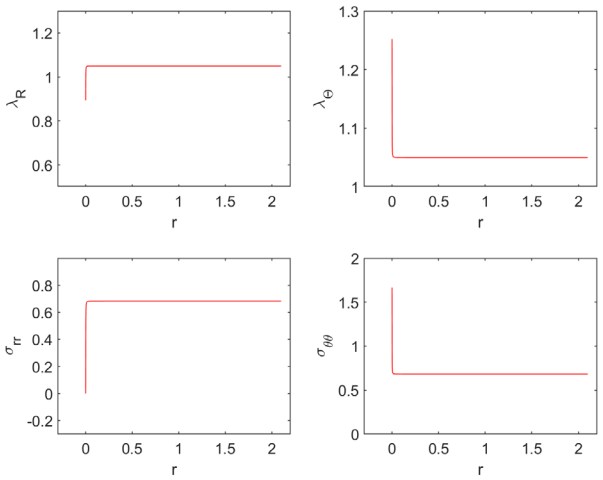

Figure 3. Stresses and strains of a membrane with an undeformed hole size radius of 0.001 and an outer radius of 2.0 extended by 5% using parameter values c_{01}=0.9, c_{10}=0.2, and c_{20}=0.5

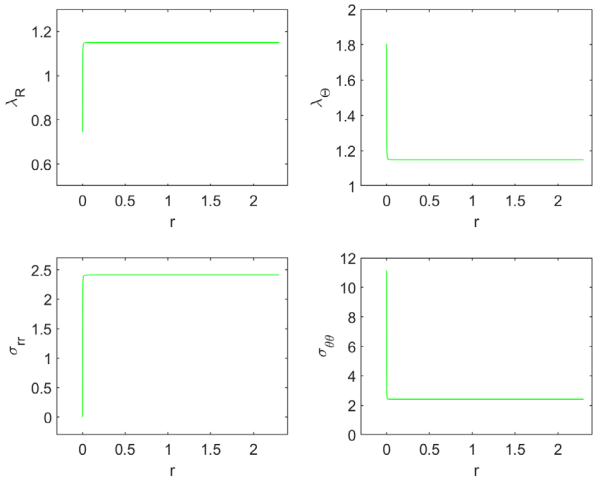

Figure 5. Stresses and strains of a membrane with an undeformed hole size radius of 0.001 and an outer radius of 2.0 extended by 15% using parameter values c_{01}=0.9, c_{10}=0.2, and c_{20}=0.5

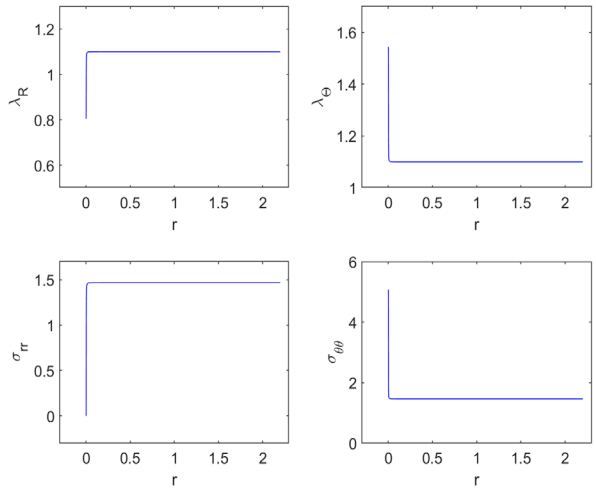

Figure 4. Stresses and strains of a membrane with an undeformed hole size radius of 0.001 and an outer radius of 2.0 extended by 10% using parameter values c_{01}=0.9, c_{10}=0.2, and c_{20}=0.5

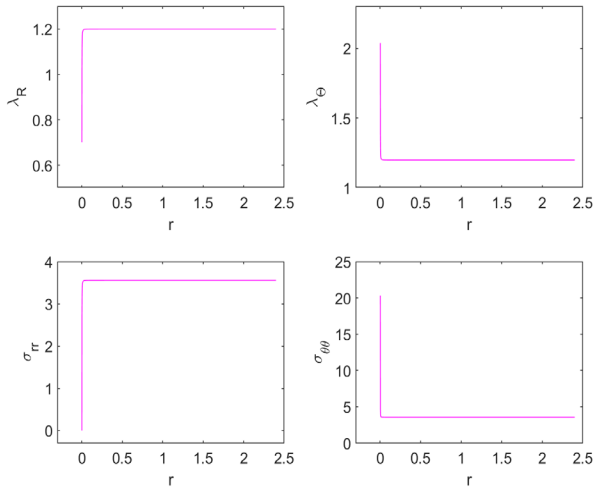

Figure 6. Stresses and strains of a membrane with an undeformed hole size radius of 0.001 and an outer radius of 2.0 extended by 20% using parameter values c_{01}=0.9, c_{10}=0.2, and c_{20}=0.5

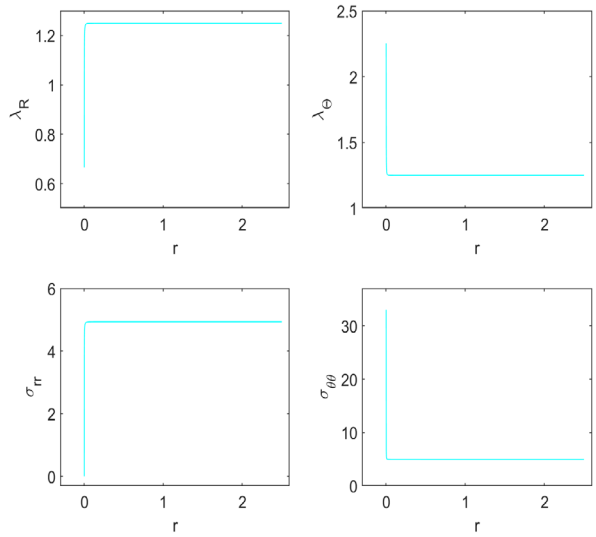

Figure 7. Stresses and strains of a membrane with an undeformed hole size radius of 0.001 and an outer radius of 2.0 extended by 25% using parameter values c_{01}=0.9, c_{10}=0.2, and c_{20}=0.5

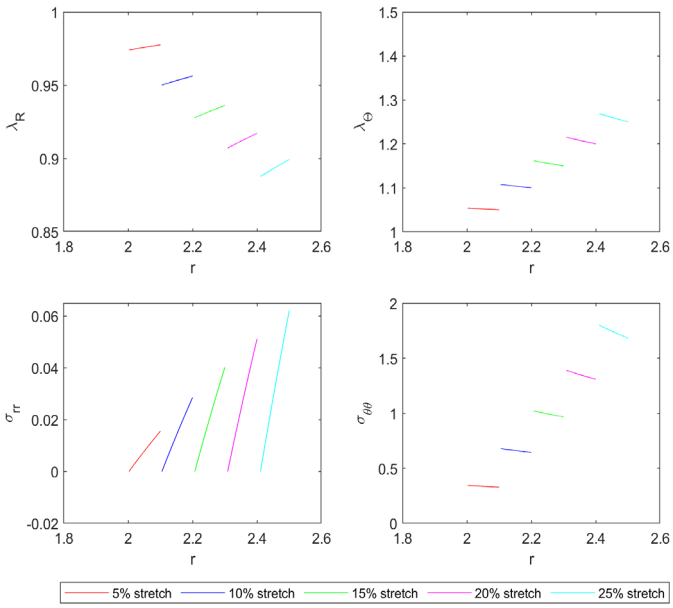

Figure 8. Stresses and strains of a membrane with an undeformed hole size radius of 1.9 and an outer radius of 2.0 extended by 5%, 10%, 15%, 20%, and 25% using parameter values c_{01}=0.9, c_{10}=0.2, and c_{20}=0.5

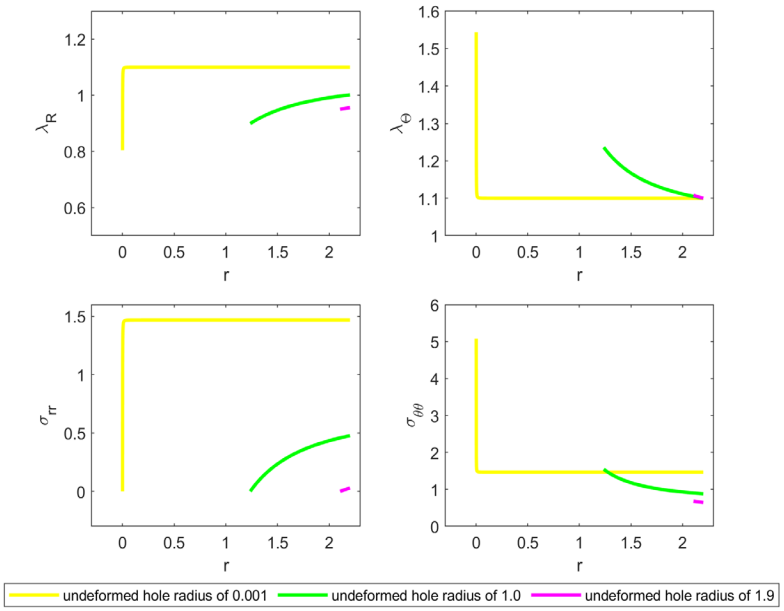

Figure 9. Results for three membranes with undeformed hole radii of 0.001, 1.0, and 1.9 and an outer radius of 2.0 extended by 10% using parameter values c_{01}=0.9, c_{10}=0.2, and c_{20}=0.5

DISCUSSION

The aim of the present study is to examine the behavior of a circular Mooney-Rivlin membrane with a central circular hole when the outer boundary is stretched. Even though results of this study showed that the stresses and strains of the materials used in this study exhibit the same behavior (monotonically increasing or decreasing) regardless of material, it is important to note that there is a high stress concentration near the hole when the hole size is small, whereas a membrane with a larger size hole will have lower stresses near the hole. Moreover, stretching the membrane further increases the stress at the boundaries. The results are qualitatively

comparable to the results of David and Humphrey (2004) when considering the isotropic cases.

Since the present study is limited only to the three-parameter Mooney-Rivlin model, it is important to investigate further the kinematics of a membrane behaving under a Mooney-Rivlin model with a higher number of parameters, and in cases when the central hole may be elliptical. However, present results can serve as important guide to future studies in the field of mechanics and medicine.

As stated in the introduction, results of this study are helpful in guiding surgeries and clinical procedures. As the world of medicine move to procedures and surgeries where only small incisions are needed, it is important to know how this introduction of small holes affect the stress and strain fields of cells in our body.

ACKNOWLEDGEMENT

This work is supported by a grant from the Department of Science and Technology – Science Educational Institute under the Accelerated Science and Technology Human Resource Development Program.

LITERATURE CITED

Bansal, RK. 2007. Solid and Fluid Mechanics, 2nd Edition. New Delhi: Laxmi Publications (P) Ltd. 322-323 pp.

Benkahla J, Baranger TN, Issartel J. 2012. Experimental and numerical simulation of elastomeric outsole bending. Exp Mech 52: 1461-1473.

Benkahla, J, Baranger, TN, Issartel, J. 2013. Fatigue life estimation for an NBR Rubber and an expanded polyurethane. Exp Mech 53: 1383-1393.

Bonet, J, Wood, RD. 1997. Nonlinear Continuum Mechanics for Finite Element Analysis. Cambridge, UK: Cambridge University Press.

David, G, Humphrey JD. 2004. Redistribution of stress due to a circular hole in a nonlinear anisotropic membrane. J. Biomech 37(8):1197-1203.

David, G, Humphrey JD. 2007. Finite element model of stresses in the anterior lens capsule of the eye. Comput Methods Biomech Biomed Engin 10(3):237-243.

David, G, Nabong JR. 2015. Rupture model of intracranial saccular aneurysms due to hypertension. J Mech Med Biol 15 (03): 1550022.

Maurice, X, Sandholm A, Pronost, N, Boulic, R, Thalmann, D. 2009. A subject-specific software solution for the modeling and the visualization of muscles deformations. Vis Comput 25: 835-842.

Mori, D, David, G, Humphrey, JD, Moore Jr., JE. 2005. Stress distribution in a circular membrane with a central fixation. J Biomech Eng 127: 549-553.

Nabong, JR, David, G. 2017. Finite element model of size, shape and blood pressure on rupture of intracranial saccular aneurysms. J Phys Conf Ser 893(1): 012054.

Rivlin, RS, Thomas, AG. 1951. Large elastic deformations of isotropic materials VIII. Strain distribution around a hole in a sheet. Philosophical Transactions of the Royal Society (London) A 243: 289-298.

Shabana, AA. 2008. Computational Continuum Mechanics. Cambridge, UK: Cambridge University Press.

Verron, E, Andriyana A. 2008. Definition of a new predictor for multiaxial fatigue crack nucleation in rubber. J Mech Phys Solids 56: 417-443.

Xu, X, Sun L, Fan X. 1995. Stress concentration of finite composite laminates with elliptical hole. Comput Struct 57(1): 29-34.

Authors: Michele O. Olivares, *Division of Physical Sciences and Mathematics, College of Arts and Sciences, University of the Philippines Visayas, Miagao (5023), Iloilo*
e-mail: moolivares@up.edu.ph

Guido David, *Institute of Mathematics, University of the Philippines Diliman*
e-mail: gdavid@math.upd.edu.ph